# Separation of halloysite/kaolinite mixtures in water controlled by sucrose addition: the influence of the attractive forces on the sedimentation behaviour

Martina Maria Calvino, Giuseppe Cavallaro*, Lorenzo Lisuzzo, Stefana Milioto, Giuseppe Lazzara

*Dipartimento di Fisica e Chimica, Università degli Studi di Palermo, Viale delle Scienze, pad. 17, 90128 Palermo, Italy. giuseppe.cavallaro@unipa.it*

**Keywords:** Halloysite nanotubes, Nanoclays, Aqueous colloidal stability, Separation, TGA

## Abstract

In this work, we propose an easy strategy for the separation of halloysite/kaolinite mixtures in sucrose aqueous solution. Preliminarily, we investigated the influence of the sucrose addition on the colloidal stability of kaolinite nanoplates and halloysite nanotubes (HNTs) dispersed in water. Dynamic Light Scattering (DLS) measurements revealed that the HNTs aqueous mobility is dependent on the sucrose concentration, while the ζ-potential is negligibly affected by the addition of the carbohydrate in the aqueous solvent. On the other hand, any variations on the surface charge and dynamic behaviour of kaolinite were detected in the presence of sucrose. The obtained ζ-potential and DLS results were useful to interpret the sedimentation kinetics of kaolinite and halloysite dispersions. In particular, the peculiar sedimentation behaviour of halloysite were discussed by considering the screening effect of sucrose on the attractive interactions between the nanotubes. The latter was evaluated by the calculation of the corresponding Hamaker constants. On this basis, we estimated that the optimization of the separation between kaolinite and halloysite might be achieved in 10 wt% sucrose aqueous solution. This hypothesis was confirmed by the separation experiments, which exploited the different sedimentation behaviour of halloysite and kaolinite. Thermogravimetric experiments on the separated material and kaolinite/halloysite composites with variable composition allowed us to determine the efficiency of the separation protocol. To this purpose, the differential thermogravimetric curves were accurately analysed by using split Gaussian functions.

In conclusion, this paper represents a further step in the purification of natural halloysite samples exploiting the ability of sucrose to control the attractive forces of the clay nanotubes as well as the colloidal stability of kaolinite nanoplates in aqueous solvent.

## 1. Introduction

Nowadays, nanoclays are receiving the attention of researchers in several fields, including material sciences [1–3], engineering [4–6] and biology [7–10] due to their physico-chemical properties, environmental-friendly nature and low cost [11].

Among the clay nanoparticles, halloysite nanotubes (HNTs) have attracted particular interest. They are aluminosilicates characterized by a chemical formula of $Al_2Si_2O_5(OH)_4 \cdot nH_2O$ and a hollow tubular structure with a spiral conformation [12]. Halloysite is formed by rolling-up a kaolin double layer yielding a tubular structure. Their sizes depend on the geological deposit. Averagely, the tubes' length range within 0.5-1.5 μm and the outer diameter is between 50-100 nm, whereas for internal diameter of the cavity is from 10 to 20 nm.

The external surface is composed of Si-O-Si groups and the internal lumen surface of Al-OH. In light of this and considering the charges of alumina and silica substrates, it is observed a charge separation in the pH range between 2 and 8 [13], in particular the inner lumen carries a positive charge, while the outer surface is negatively charged [14]. Inner and outer surfaces can be selectively modified by exploiting covalent and supramolecular interactions [15–18]. Accordingly, halloysite nanotubes have been developed as carriers for controlled release of active agents [19–32], as fillers for polymers [33–39] and for decontamination purposes [40–45]. Due to its high specific surface, halloysite was used as catalytic support for technological applications [46–54]. Recently, halloysite was successfully employed for the protective coating of hair [55,56]. The chemical composition of halloysite is similar to that of kaolinite except for the presence of water molecules between the unit layers. Similarly to halloysite, kaolinite has been exploited in many fields as inorganic support with adsorption application [57,58] or as precursor in geopolymeric materials [59,60].

Typically, halloysite samples are contaminated by a certain amount (ca. 10 wt%) of platy kaolinite nanoparticles depending on the deposit [61]. This aspect might be relevant for some applications where the high purity of halloysite is requested. As example, the presence of kaolinite nanoplates can

reduce the efficiency of HNT as nanocarriers for pharmaceutical and biomedical applications. To the light of this consideration, the development of separation protocols for halloysite samples represents a challenging task for their applications in pharmaceutics and biomedicine.

According to literature, the sedimentation behaviour of nanoparticles in a colloidal systems depends on several factors, including the specific interactions as well as the viscosity and the ionic strength of the solvent [62–64] that can induce aggregation decreasing the colloidal stability. The separation of kaolinite nanoplates can be favoured by adding inorganic flocculants [65], such as aluminium and iron salts or other greener flocculants [66]. Moreover, the addition of polymers can influence the sedimentation kinetics of kaolinite dispersed in water [67].

In this work, we investigated the effects of sucrose addition on the colloidal stability of halloysite and kaolinite in aqueous media. Specifically, the screening effect of sucrose towards the attractive interactions between the clay nanotubes was studied according to the DLVO theory. In this regard, it should be noted that the addition of variable amounts of monosaccharides (glucose) or disaccharides (sucrose and maltose) represents an efficient strategy to control the stability of aqueous dispersions because of their influence on the physico-chemical properties (dielectric constant, refractive index and viscosity) of water [68]. The effects of sugars on the attractions between dispersed nanoparticles can be evaluated according to the Hamaker constant. On the other hand, the addition of non ionic macromolecules (such as polymers and surfactants) can be affect the aqueous colloidal stability of nanoclays due to steric interactions and depletion processes as reported for kaolinite dispersions containing variable amounts of biopolymer [67].

In conclusion, the influence of sucrose concentration on the sedimentation kinetics of both nanoclays was investigated in order to maximize the separation efficiency in halloysite/kaolinite aqueous mixtures. The obtained results can be useful to develop purification protocols for natural halloysites.

## 2. Materials and methods

## 2.1 Materials

Halloysite nanotubes (HNTs) were provided by Imerys Ceramics. They are from Matauri Bay (New Zealand). The HNTs possess a specific surface area of 28.6 $m^2 g^{-1}$ [61]. Their length range between 100 to 3000 nm, while the intervals for the inner and outer diameters are 15-70 and 50-200 nm, respectively [33]. Compared to halloysite obtained from Dragon Mine [61], the employed HNTs do not contain impurities of kaolinite. Kaolinite (Kao) and sucrose (purity ≥ 99.5%) are Sigma Aldrich products. Water from reverse osmosis (Elga model Option 3) with a specific resistivity greater than 1MΩ cm was used.

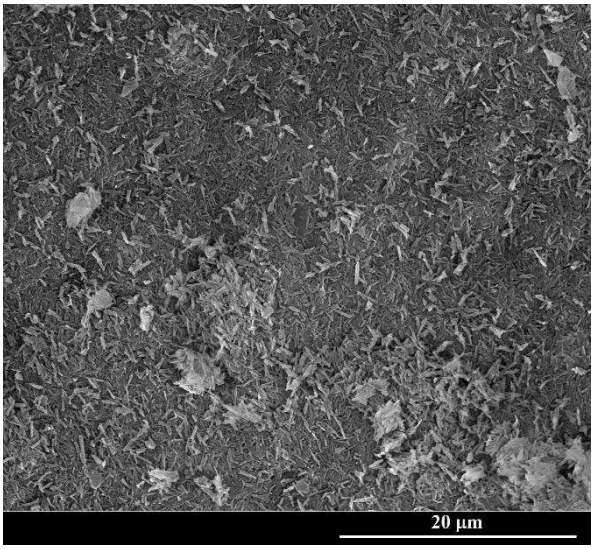


**Figure. 1.** SEM image of halloysite nanotubes

## 2.2 Preparation of dispersions

As concerns sedimentation experiments, halloysite nanotubes and kaolinite (concentration of 2 wt%) were separately added to 5 mL of sucrose solutions with variable concentration ranging from 1 to 35 wt%.

The obtained dispersions were sonicated for 15 minutes, magnetically stirred for 2 hours and equilibrated for 2 hours to monitor the colloidal stability of the nanoparticles.

Dynamic Light Scattering (DLS) and ζ-potential tests were conducted on HNTs or kaolinite dispersed in sucrose solutions at variable concentration. The dispersions were prepared by 15 minutes of sonication followed by 2 hours of magnetically stirring.

### 2.3 Separation of halloysite/kaolinite mixtures

Separation experiments of halloysite/kaolinite mixtures were conducted as reported below. Firstly, we prepared halloysite/kaolinite mixtures with a 1:1 mass ratio in 10 wt% sucrose aqueous solution. The concentration of both nanoclays was fixed at 2 wt%. The dispersion was sonicated for 15 minutes, magnetically stirred for 2 hours and equilibrated for 30 minutes, which does not guarantee the complete sedimentation of the nanoparticles. Then, we removed the upper part of the dispersion corresponding to 30% of the total volume. Then, the recovered suspension was dried at 50 °C. Finally, the dried powder was washed five times with water to remove sucrose and then, stored in a desiccator at 25 °C and relative humidity of 75 %. For comparison, the separation experiment was conducted using water as solvent.

### 2.4 Methods

The refractive indexes (RI) of the sucrose solutions were determined through an automatic refractometer (Model GPR 11-37, Index Instruments). Sample amounts were directly placed into the instrument cell where they were left to equilibrate. All measurements were performed at 25.0 ± 0.1 °C.

The viscosity experiments were carried out by using an Ubbelohde viscosimeter, which was aligned perpendicularly in a plexiglass box with circulating water (thermostatted with a Haake D8 apparatus). The absolute viscosity (η) of the sucrose solutions were estimated at 25.0 ± 0.1 °C.

The dielectric constant of sucrose solutions was determined by means of a Hewlett-Packard impedance analyzer (HP 4294A) equipped with HP 16451B dielectric test fixtures. The experiments were conducted at 25 ± 0.1 °C.

ζ-potential and dynamic light scattering (DLS) measurements on the nanoclay aqueous dispersions were performed by a Zetasizer NANO-ZS (Malvern Instruments) at 25 ± 0.1 °C. °C. For ζ-Potential experiments a disposable folded capillary cell was used. As concerns DLS experiments, the field-time autocorrelation functions were described by a mono-exponential decay which provides the decay rate (Γ) of the diffusive mode. For the translational motion, the diffusion coefficient at a given concentration is $D_t = \Gamma/q^2$ where q is the scattering vector given by $4\pi n\lambda^{-1}\sin(\theta/2)$ being n the refractive index, λ the wavelength (632.8 nm) and θ the scattering angle (173°).

The sedimentation experiments were carried out in glass tubes of ca. 2 cm in diameter and length of ca. 6 cm. The kaolinite and halloysite dispersions were imaged in fixed intervals of time for 2 hours. Then, the sedimentation volume and the settling velocity of the two clays in sucrose solutions were obtained from the sedimentation front, which was determined by using ImageJ software.

Thermogravimetric experiments were performed by using a Q5000 IR apparatus (TA Instruments) under inert atmosphere. To this purpose, the measurements were conducted under nitrogen flows of 25 and 10 $cm^3$ $min^{-1}$ for the sample and the balance, respectively. Tests were carried out by heating the sample from room temperature to 700 °C with a heating rate of 20°C $min^{-1}$. TGA analyses were conducted on the materials obtained from the separation of halloysite/kaolinite mixtures. In addition, TG experiments were performed on halloysite/kaolinite composites at variable composition and their pristine components. The temperature calibration of the apparatus was conducted on the basis of the Curie temperatures of standards as reported in literature [69,70].

Scanning electron microscopy (SEM) was conducted using a microscope ESEM FEI QUANTA 200F. Prior to the experiment, the surface of the clays was coated with gold in argon by means of an Edwards Sputter Coater S150A to avoid charging under electron beam. The analyses were carried

out in high vacuum mode (< 6 × 10-4 Pa) for simultaneous secondary electron; the energy of the beam was 25 kV and the working distance was 10 mm.

## 3. Results and Discussion

### *3.1. Properties of the sucrose solutions*

Preliminarily investigations on the sucrose solutions were conducted for a proper analysis and interpretation of the colloidal behaviour of the nanoclay dispersions. The obtained results are presented in Table 1. It should be noted that the investigated properties affect the electrophoretic mobility, the aqueous dynamic characteristics and the sedimentation properties of the nanoparticles dispersed in the aqueous sucrose solutions.

**Table 1.** Refractive index, relative dielectric constant and viscosity of sucrose solutions in water at 25 °C.

| Sucrose concentration / wt % | RI | $\varepsilon_r$ | $\eta$ / mPa s |
|---|---|---|---|
| 0 | 1.3325 | 78.4 | 0.8891 |
| 1.27 | 1.3363 | 78.2 | 1.028 |
| 2.52 | 1.3379 | 77.9 | 1.055 |
| 4.8 | 1.3405 | 77.4 | 1.146 |
| 9.88 | 1.3491 | 76.1 | 1.336 |
| 15.5 | 1.3568 | 74.7 | 1.592 |
| 25.9 | 1.3702 | 72.0 | 2.175 |

### *3.2 Effects of sucrose on the aqueous diffusion behaviour and surface charge of clay nanoparticles*

The influence of sucrose addition on the aqueous diffusion coefficient of both HNTs and kaolinite was explored by Dynamic Light Scattering. As a general result, we detected that kaolinite possess lower diffusion coefficients in the aqueous solvents compared to those of halloysite (Figure 2).

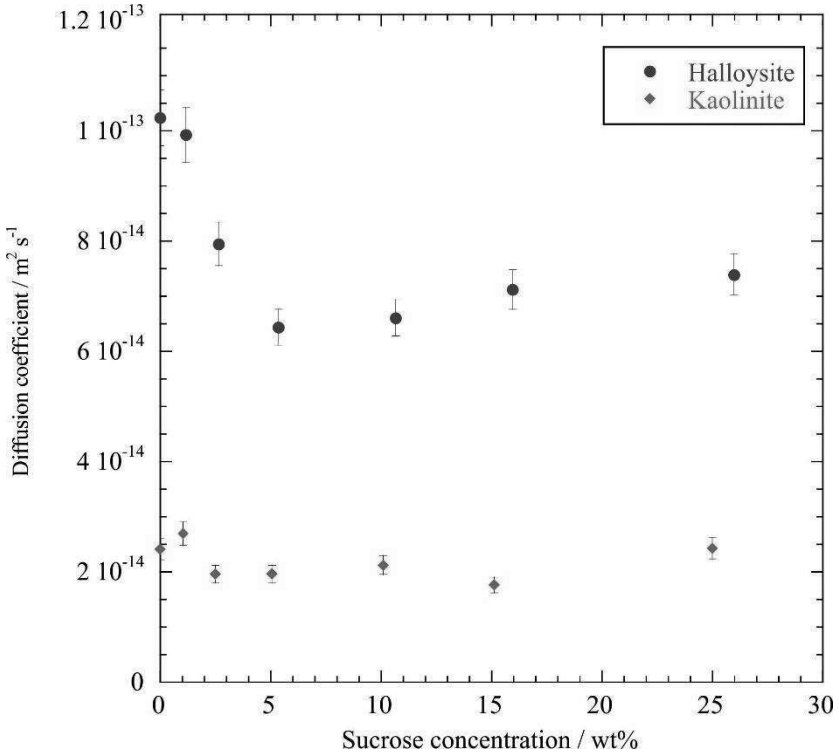


**Figure**. **2.** Aqueous diffusion coefficients of HNTs and kaolinite as functions of sucrose concentration.

These findings can be related to the larger sizes of kaolinite nanoparticles and their consequent reduced mobility in water with respect to that of HNTs. We observed that the sucrose addition does not affect the diffusion coefficient of kaolinite. On the other hand, the aqueous mobility of HNTs is significantly influenced by the presence of sucrose in the medium. As shown in Figure 2, the addition of small amounts of sucrose (concentration up to ca. 5 wt%) induced a decrease of the diffusion coefficient of halloysite indicating that the dynamic behaviour of the nanotubes was reduced. Oppositely, the further addition of sucrose generated a slight increase of the diffusion coefficient highlighting that the diffusivity of HNTs was enhanced. These trends can be related to the peculiar influence of sucrose on the interactions between the halloysite nanotubes dispersed in water. As shown by ζ-potential results (Table 2), the presence of sucrose slightly alters the surface charge of HNTs as well as kaolinite.

**Table 2.** ζ-potential of halloysite and kaolinite in sucrose solutions at variable concentration.

| Sucrose concentration / wt % | ζ-potential / mV | |
|---|---|---|
| | Halloysite | Kaolinite |
| 0 | -34.1 ± 1.5 | -21.9 ± 1.1 |
| 4.8 | -32.6 ± 1.1 | -21.3 ± 1.5 |
| 9.88 | -32.4 ± 1.4 | -22.0 ± 1.2 |
| 15.56 | -32.3 ± 1.3 | -22.3 ± 1.2 |

Based on the data in Table 2, we can state that the electrostatic repulsions between the kaolinite nanoparticles in sucrose solutions are comparable to those in water. As concerns HNTs, we observed a slight decrease of the absolute ζ-potential value in the presence of sucrose. It should be noted that the ζ-potential are negative within the whole sucrose concentration range. In general, the ζ-potential values of halloysite are more negative with respect to those of kaolinite for all the investigated sucrose concentrations. Compared to kaolinite nanoplates, halloysite nanotubes exhibited stronger repulsive interactions hindering their aggregation.

It is important to evidence that the presence of sucrose can affect the Van Der Waals interactions between the nanoparticles. Specifically, the sucrose addition can reduce the attractive interactions between the dispersed nanoclays altering the colloidal stability of the dispersions. These effects are dependent on the sucrose concentration as suggested by the results on the aqueous diffusion coefficient of halloysite (Figure 2). The influence of the sucrose concentration on the Van der Waals attractive interactions between HNTs will be extensively discussed in the paragraph 3.3.

*3.2 Sedimentation of clay nanoparticles dispersed in sucrose solutions.*

As shown in Figure 3, kaolinite and halloysite dispersions possess different macroscopic characteristics, which depend on the sucrose concentration as well as on the equilibration time after the preparation.

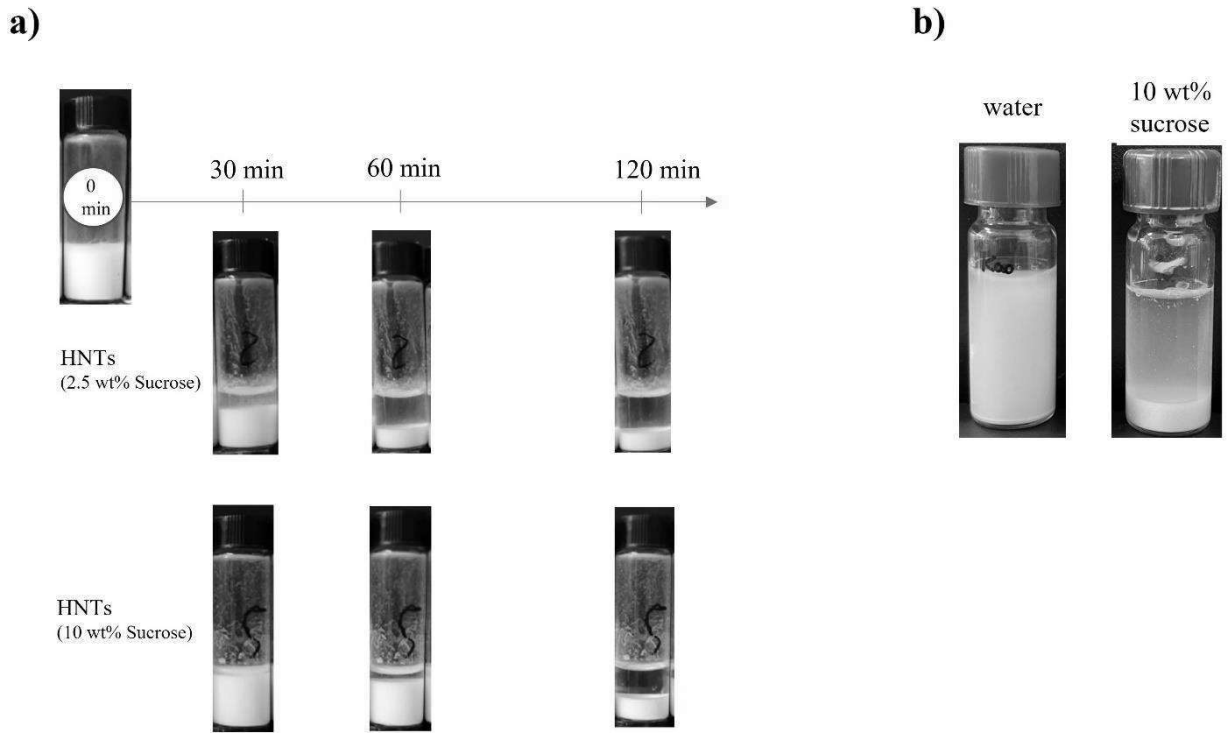


**Figure 3.** (a) Images of HNTs dispersions in 2.5 and 10 wt% sucrose at variable times of equilibration. (b) Images of kaolinite dispersions in water and 10 wt% sucrose after 30 minutes of equilibration.

Based on the images reported in Figure 3a, we observed that the increase of the sucrose concentration from 2.5 to 10 wt% slowed down the lowering of the sedimentation front in the halloysite dispersions. Accordingly, we can state that the kinetics of the HNTs sedimentation is faster for the lower sucrose concentration. The complete separation between the dispersed nanoparticles and the solvent was detected after 2 hours of equilibration for both sucrose concentrations. Figure 3b displays the kaolinite suspensions after 30 minutes of equilibration. We observed that kaolinite dispersed in water does not evidence a clear sedimentation front between the sediment and the supernatant. This observation is valid for all the kaolinite dispersions with sucrose concentration lower than 10 wt%.

In order to quantitatively describe the sedimentation kinetics, we analyzed the time evolution of the sedimentation profiles of HNTs and kaolinite dispersions through ImageJ software. In detail, we determined the sedimentation volume fraction after 2 hours of equilibration once the process is certainly complete. Moreover, we estimated the settling velocity from the slope of the sedimentation front vs time plot as reported in our previous work regarding the effect of the ionic strength on the aqueous colloidal stability of several halloysites [62]. Based on the macroscopic observations (Figure 4b), the settling velocity for kaolinite can be determined only in aqueous media containing sucrose with a concentration ≥ 10 wt%.

Figure 4a shows that sedimentation volume fraction values of kaolinite are lower than those of halloysite and they are almost constant throughout the investigated sucrose concentration range. As a general result, the kaolinite sedimentation is faster compared to that of halloysite for sucrose ≥ 10 wt% as evidenced by the settling velocity data (Figure 4b). It is remarkable to evidence that the different sedimentation kinetics could be useful for a proper separation of kaolinite and halloysite in natural samples containing both nanoclays. The addition of the carbohydrate did not alter neither the sedimentation volume fraction nor the settling velocity (for sucrose ≥ 10 wt%) of kaolinite dispersions. In contrast, the presence of sucrose affected the sedimentation kinetics of halloysite nanotubes dispersed in water. We detected that the velocity of the HNTs sedimentation is enhanced for sucrose concentration up to 5 wt%, while a further addition of sucrose generated the opposite effect. Similarly, the sedimentation volume fraction presents a minimum value at 5 wt%. The relation between the sedimentation parameters and the sucrose concentration (Figure 4) are consistent with the DLS data, which evidenced that the HNTs diffusion in water is reduced for small concentrations of sugar reaching a minimum value at 5 wt% of carbohydrate.

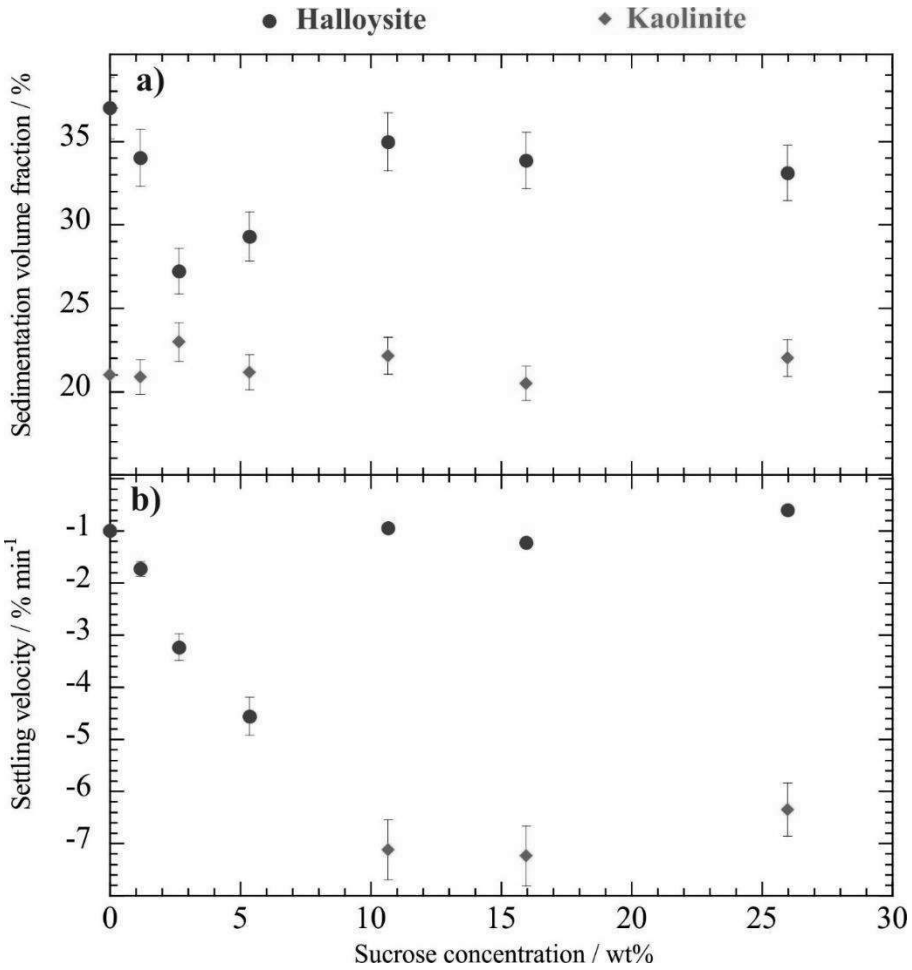


**Fig**ure **4.** Sedimentation volume fraction (a) and settling velocity (b) as functions of the sucrose concentration for halloysite and kaolinite dispersions.

*3.3 Sedimentation kinetics of halloysite: the influence of sucrose addition on the Van der Waals interactions*

The influence of the sucrose concentration on the sedimentation parameters can be discussed in terms of balance between Van der Waals forces and repulsive interactions between the nanoparticles (DLVO theory). It should be noted this approach is not suitable for the description of the kaolinite sedimentation because of the large sizes of the nanoparticles. Accordingly, DLS experiments at variable sucrose concentration evidenced that the hydrodynamic diameter of kaolinite ranges between 1828 ± 146 nm and 2796 ± 223 nm. These values were determined at sucrose concentrations equal to 1.27 and 15.5 wt%, respectively. As expected, the addition of sucrose generated slight

variations of the surface charge of HNTs (Table 2). Therefore, we can conclude that the presence of sucrose does not affect the repulsive interactions between the halloysite nanotubes. On the other hand, we can predict that the Van der Waals attractive forces are influenced by sucrose. In this regard, we calculated the Hamaker constant vs sucrose concentration for HNTs dispersions by the following equation

$$A_H = \frac{3}{4}k_B T \cdot \left(\frac{\varepsilon_1-\varepsilon_2}{\varepsilon_1+\varepsilon_2}\right)^2 + \frac{3h\upsilon_e}{8\sqrt{2}} \cdot \frac{(n_1^2-n_2^2)}{(n_1^2+n_2^2)\cdot\left(2\cdot\sqrt{n_1^2+n_2^2}\right)} \quad (1)$$

where $k_B$ is the Boltzmann constant, T is the absolute temperature, ε is the dielectric constant, n is the refractive index and $\upsilon_e$. is the mean ionization frequency of the material and it is ≈ $3.10^{15}$ Hz $10^{15}$. Here, the subscript 1 and 2 refer to halloysite and sucrose solution, respectively. Figure 5 reports the Hamaker constant function normalized by the thermal energy ($k_bT$) for halloysite nanotubes dispersed in aqueous solvent containing variable amounts of sucrose. To this purpose, we considered the fitted curves for the dielectric constant and the refractive of index of aqueous solutions with variable sucrose concentration (see Supplementary Materials).

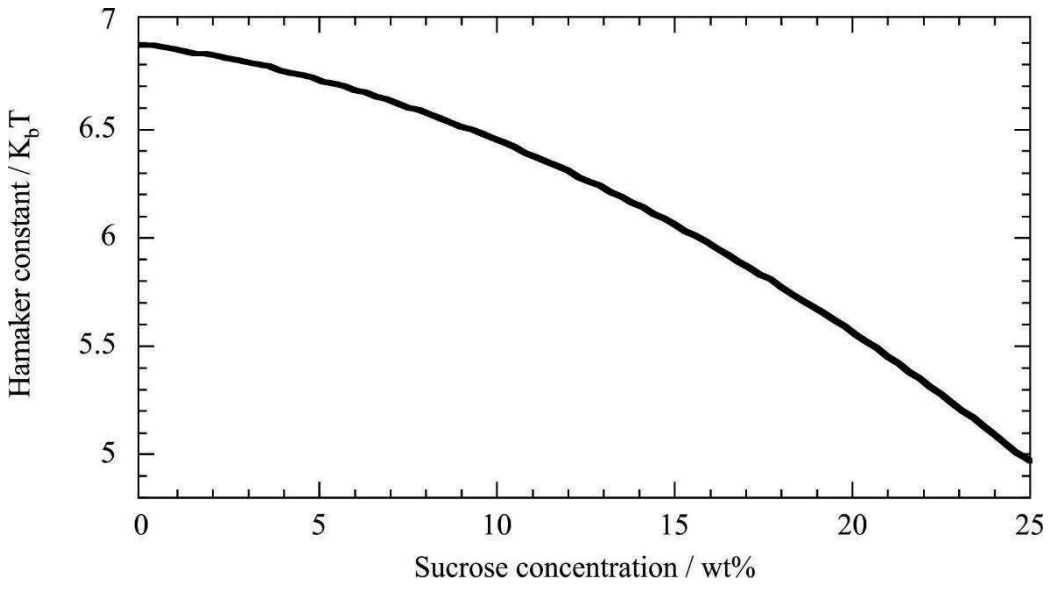


**Figure 5.** Dependence of the Hamaker constant for HNTs on the sucrose concentration. The function was calculated on the basis of equation 1 and taking into account the fitted curved for the dielectric constant and the refractive of index of sucrose aqueous solutions (see Supplementary Materials).

As shown in Figure 5, the Hamaker constant is positive for all the sucrose concentrations indicating that the Van der Waals forces are attractive. We observed that the sucrose addition decreases the attractive forces between the nanotubes dispersed in water. In other words, the reduction of the Hamaker constant agrees with the screening of the Van der Waals interactions between the dispersed nanotubes. This effect is enhanced by increasing the sucrose amount in the aqueous medium. The decreasing trend of the Hamaker constant on the sucrose concentration (Figure 5) can be described by a binomial equation within the whole investigated range. Interestingly, a linear region with slight variations of the Hamaker constant can be identified for sucrose $\leq$ 5 wt%. In detail, we estimated that the reduction of the Hamaker constant is lower than 2% highlighting that the influence of sucrose on the attractions between the nanoparticles is negligible for sugar concentration up to ca. 5 wt%.

Based on these considerations, we can hypothesize that the attractive forces are largely predominant with respect to the repulsions in the presence of small amounts of sucrose and, consequently, the clustering between HNTs is favoured. Accordingly, the aqueous diffusion coefficient decreased (Figure 2) and the sedimentation kinetics was enhanced (Figure 4b). These results are also consistent with the slight reduction of the HNTs surface (Table 2). On the other hand, the discrepancy between attractions and repulsions was reduced for sucrose concentration $\geq$ 10 wt% explaining both DLS data and the sedimentation parameters. Namely, the attractive forces are significantly screened by sucrose determining an increase of the aqueous mobility and an improvement of the colloidal stability of the nanotubes.

*3.4 Separation of halloysite and kaolinite in sucrose solution*

Generally, natural clay samples are mixtures of different minerals limiting their use for several purposes. Within this, it should be noted that natural halloysites can contain variable amounts of kaolinite. Therefore, the successful separation of halloysite and kaolinite is crucial to make HNTs suitable for technological applications. Here, we exploited their sedimentation kinetics in sucrose

solutions to obtain an efficient separation of the two nanoclays in halloysite/kaolinite mixtures. The protocol used for the separation of halloysite and kaolinite is described in the paragraph 2.3. Scanning electron microscopy evidenced the co-presence of few kaolinite nanoplates and a large amount of halloysite nanotubes in the sample obtained from 10 wt% sucrose solution (see Supplementary Materials). The efficiency of the separation procedure was estimated by thermogravimetry, which is a powerful technique for the quantitative and qualitative characterization of multicomponent materials [1,71]. Figure 6 compares the differential thermogravimetric curves of pristine nanoclays and their mixture (HNT/Kaolinite 50:50) with those of the materials obtained by the separation through both water and 10 wt% sucrose solution. According to literature [72,73], pure halloysite exhibited the main mass loss in the temperature range between 400 and 600 °C due to expulsion of the interlayer water molecules, while kaolinite evidenced a significant mass reduction in a broader range (between 480 and 700 °C). On this basis, we focused the analysis of the differential thermogravimetric curves of the separated materials within the range 400-700 °C.

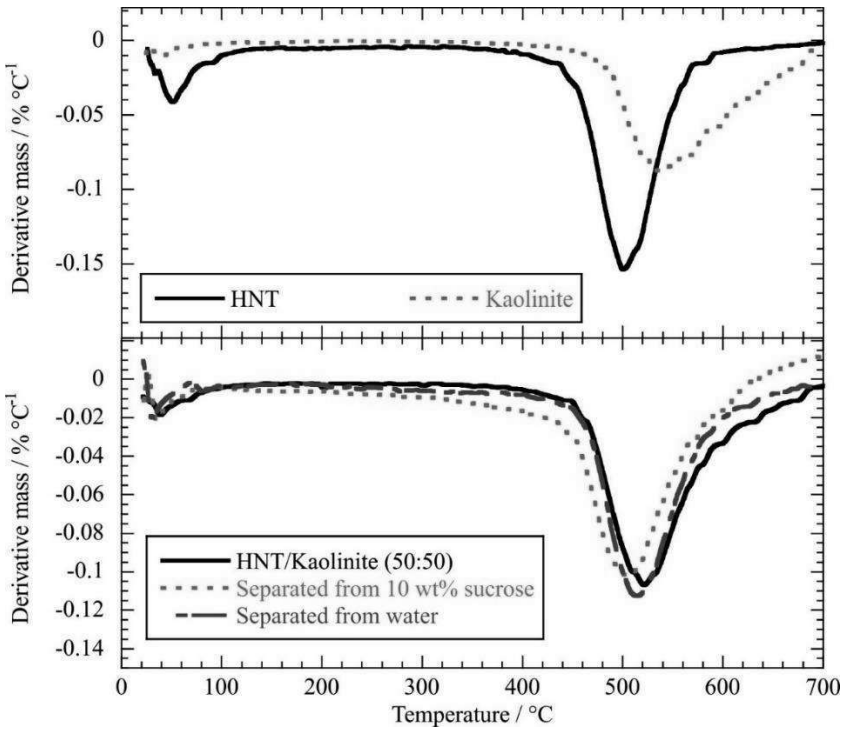


**Figure 6.** Differential thermogravimetric curves of kaolinite, halloysite, kaolinite/halloysite (50:50) mixture and the materials obtained from the separation in water and 10 wt% sucrose solution.

Firstly, we determined the peak temperatures ($T_{peak}$) for the different samples from the minimum of the differential thermogravimetric curves. As shown in Supplementary Materials, a linear function was detected for the dependence of $T_{peak}$ on the composition of halloysite/kaolinite mixtures. Based on the linear fitting of this trend, we calculated the mass percent of halloysite in the separated materials from the corresponding $T_{peak}$ values (503.8 and 514.8 °C from sucrose solution and water, respectively). We determined that the halloysite contents are 97 ± 3 wt% and 59 ± 3 wt% for the materials obtained from the separation through 10 wt% sucrose solution and water, respectively.

A more accurate analysis was conducted by the fitting of the DTG curves using Fityk software [74]. The split Gaussian function was used as model for the analysis of the DTG curves. As shown in Supplementary Materials, DTG curves of both pristine kaolinite and halloysite were fitted using the split Gaussian equation, which can be expressed as

$$dm/dT = (dm/dT)^{*} \cdot \exp[-\ln(2) \cdot (T - T_C)/\Delta T_L)^2 \quad \text{for } T \leq T_C \tag{2}$$

and

$$dm/dT = (dm/dT)^{*} \cdot [-\ln(2) \cdot (T - T_C)/\Delta T_R)^2 \quad \text{for } T \geq T_C \tag{3}$$

where $T_C$ is the temperature at the center of the function, $\Delta T_L$ and $\Delta T_R$ are the left and right widths indicated as temperature ranges, while $(dm/dT)^{*}$ is the common value for the left and right sides.

The parameters obtained by the fitting of the DTG curves of kaolinite and halloysite are reported in Supplementary Materials. The DTG curves of halloysite/kaolinite mixtures with variable composition were successfully fitted by combining the split Gaussian equations of halloysite and kaolinite. Specifically, $(dm/dT)^{*}$ for halloysite and kaolinite contributions were considered as fitting parameters, while $T_C$, $\Delta T_L$ and $\Delta T_R$ for both nanoclays were fixed (the values determined by the fitting of the DTG curves of pristine HNT and kaolinite). As example, Figure 7a compares the experimental and calculated DTG curves for the mixture composed by 50 wt% of halloysite. In

addition, Figure 7b shows separately the split Gaussian functions combined for the fitting analysis. Based on the fitted DTG curves, we can estimate the mass percent of halloysite in the mixture by using the following equation

$$HNT(wt\%)_{SGE} = 100 \cdot (A(SGE)_{HNT}/(A(SGE)_{M}) \quad (4)$$

being $A(SGE)_M$ the area obtained by the integration of the split Gaussian function of the mixture, while $A(SGE)_{HNT}$ is the integral area for the single contribution of halloysite used in the fitting analysis. Figure 7c shows a linear trend of the calculated $HNT(wt\%)_{SGE}$ values and the halloysite mass percent employed for the preparation of the mixtures. The linear fitting of the data presented in Figure 7c allowed us to determine a calibration curve for the calculation of the HNT content in halloysite/kaolinite composite samples with unknown composition including the separated material obtained by the protocol reported in the paragraph 2.3.

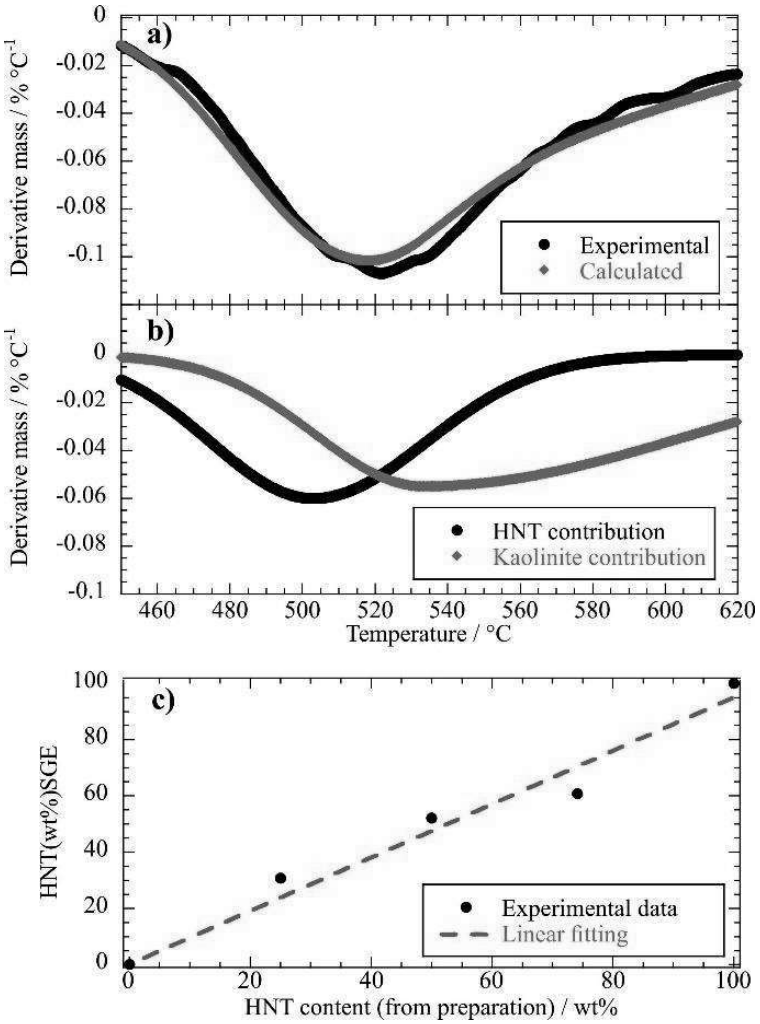


**Figure 7.** (a) Experimental and fitted DTG curves for the mixture composed by 50 wt% of halloysite. (b). Split Gaussian functions of halloysite and kaolinite employed in the fitting analysis. (c) Dependence of the halloysite content determined by the fitting (equation 4) on the HNT concentration used for the preparation of mixture with variable composition. The linear regression presents $R^2$ equals to 0.985, while the relative error for the fitting parameter (the angular coefficient) is 6%.

As evidenced in Figure 8a, the DTG curve of the sample separated from sucrose solution can be analyzed by using the combination of the split Gaussian equations of halloysite and kaolinite. Figure 8b shows that the contribution of halloysite to the fitting analysis is significantly higher compared to that of kaolinite. Based on the corresponding $HNT(wt\%)_{SGE}$ value (84.3 wt%) and the calibration curve (Figure 7c), we determined that the halloysite content in the separated material is equal to 89 ± 5 wt%, which confirms that the separation procedure in sucrose aqueous solution was very efficient. On the other hand, we determined that the sample separated from water presents a $HNT(wt\%)_{SGE}$ value of 51.6 wt%. On this basis, we calculated a HNT content equals to 53 ± 4 wt%, which is

significantly lower to that detected for the material separated from 10 wt% sucrose. According to these results, we can state that the addition of sucrose in the aqueous solvent favors the separation between the nanoclays. This finding can be related to the macroscopic observations of the dispersions (Figure 3) and the sedimentation kinetics (Figure 4), which highlighted that the addition of 10 wt% of sucrose decreases the kaolinite colloidal stability, while the settling velocity of halloysite was slightly affected.

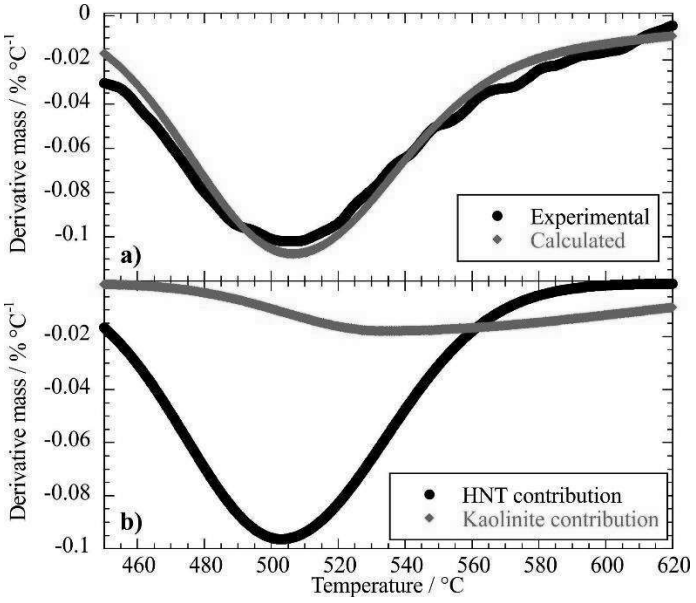


**Figure 8.** (a) Experimental and fitted DTG curves for the material obtained by the separation in 10 wt% sucrose solution. (b). Split Gaussian functions of halloysite and kaolinite employed in the fitting analysis.

## 4. Conclusions

This study was aimed to develop a novel protocol for the separation of halloysite/kaolinite mixtures by exploiting the variable effects of sucrose addition on the aqueous colloidal stability of both nanoclays. In this regard, it should be noted that the control of the nanoclays sedimentation is crucial for the purification of natural halloysite samples. Based on Dynamic Light Scattering (DLS) results, we observed that the influence of sucrose on the diffusion of halloysite nanotubes in water is dependent on the concentration of the carbohydrate, while any effects were detected for kaolinite nanoplates. As expected, the surface charge of the nanoclays is slightly influenced by the presence

of the carbohydrate. According to the DLS and ζ-potential data, we observed that small amounts of sucrose (< 10 wt%) enhanced the sedimentation kinetics of halloysite nanotubes. This effect was avoided by increase the sucrose concentration (≥ 10 wt%) in agreement with the significant screening towards the attractive interactions between the clay nanotubes. Interestingly, the dispersibility of kaolinite was strongly reduced in the presence of sucrose with a concentration larger than 10 wt%. On this basis, we evaluated that the separation efficiency of halloysite/kaolinite mixtures can be optimized in 10 wt% sucrose aqueous solution. Thermogravimetry was employed to determine the quantitative composition of the materials separated in water as well as in 10 wt% sucrose solution. The fitting analysis of the differential thermogravimetric curves by split Gaussian functions allowed us to estimate that the halloysite contents in the separated materials. We detected that the presence of 10 wt% sucrose in the aqueous medium generated a significant increase of the halloysite content (89 ± 5 wt%) in the separated material with respect to that obtained by the separation in water (53 ± 4 wt%). In conclusion, this paper demonstrated that a successful separation between halloysite and kaolinite can be achieved by the addition of sucrose in aqueous solvents. The separation efficiency can be controlled by the sucrose concentration, which influenced the aqueous colloidal stability and sedimentation kinetics of both nanoclays. Remarkably, the proposed protocol can be exploited for the purification of natural halloysite samples.

**Acknowledgments**. The authors acknowledge the University of Palermo for the financial support. The work was funded by Progetto "SETI-Sicilia Eco Tecnologie Innovative", PO FESR Sicilia 2014/2020 – Azione 1.1.5, Codice Progetto: 2017-NAZ-0204".

**Supplementary Materials.**

Fitting curves and experimental data for refractive index and dielectric constant of aqueous solutions containing variable amounts of sucrose.
Dependence of the peak temperature (determined from the minimum of DTG curves) for halloysite/kaolinite mixtures with variable composition.

Experimental and fitted DTG curves for pristine kaolinite and halloysite.
SEM image of the sample obtained from the separation in 10 wt% sucrose solution.
Fitting parameters obtained by analysis through the split Gaussian equations of the DTG curves of halloysite and kaolinite.

## References


[1] L. Lisuzzo, G. Cavallaro, S. Milioto, G. Lazzara, Halloysite nanotubes filled with MgO for paper reinforcement and deacidification, Appl. Clay Sci. 213 (2021). https://doi.org/10.1016/j.clay.2021.106231.

[2] B. Chen, J.R.G. Evans, Impact strength of polymer-clay nanocomposites, Soft Matter. 5 (2009) 3572–3584. https://doi.org/10.1039/b902073j.

[3] A. Joshi, E. Abdullayev, A. Vasiliev, O. Volkova, Y. Lvov, Interfacial modification of clay nanotubes for the sustained release of corrosion inhibitors, Langmuir. 29 (2013) 7439–7448. https://doi.org/10.1021/la3044973.

[4] E. Nyankson, O. Olasehinde, V.T. John, R.B. Gupta, Surfactant-Loaded Halloysite Clay Nanotube Dispersants for Crude Oil Spill Remediation, Ind. Eng. Chem. Res. 54 (2015) 9328–9341. https://doi.org/10.1021/acs.iecr.5b02032.

[5] R.F. Fakhrullin, Y.M. Lvov, Halloysite clay nanotubes for tissue engineering, Nanomed. 11 (2016) 2243–2246. https://doi.org/10.2217/nnm-2016-0250.

[6] Y. Feng, X. Zhou, J. Yang, X. Gao, L. Yin, Y. Zhao, B. Zhang, Encapsulation of Ammonia Borane in Pd/Halloysite Nanotubes for Efficient Thermal Dehydrogenation, ACS Sustain. Chem. Eng. 8 (2020) 2122–2129. https://doi.org/10.1021/acssuschemeng.9b04480.

[7] E. Ruiz-Hitzky, P. Aranda, M. Darder, G. Rytwo, Hybrid materials based on clays for environmental and biomedical applications, J. Mater. Chem. 20 (2010) 9306–9321. https://doi.org/10.1039/c0jm00432d.

[8] I. Guryanov, E. Naumenko, F. Akhatova, G. Lazzara, G. Cavallaro, L. Nigamatzyanova, R. Fakhrullin, Selective Cytotoxic Activity of Prodigiosin@halloysite Nanoformulation, Front. Bioeng. Biotechnol. 8 (2020). https://doi.org/10.3389/fbioe.2020.00424.

[9] M. Liu, Y. Zhang, C. Wu, S. Xiong, C. Zhou, Chitosan/halloysite nanotubes bionanocomposites: Structure, mechanical properties and biocompatibility, Int. J. Biol. Macromol. 51 (2012) 566–575. https://doi.org/10.1016/j.ijbiomac.2012.06.022.

[10] Y. Dong, S.-S. Feng, Poly(D,L-lactide-co-glycolide)/montmorillonite nanoparticles for oral delivery of anticancer drugs, Biomaterials. 26 (2005) 6068–6076. https://doi.org/10.1016/j.biomaterials.2005.03.021.

[11] M. Fizir, A. Richa, H. He, S. Touil, M. Brada, L. Fizir, A mini review on molecularly imprinted polymer based halloysite nanotubes composites: innovative materials for analytical and environmental applications, Rev. Environ. Sci. Biotechnol. 19 (2020) 241–258. https://doi.org/10.1007/s11157-020-09537-x.

[12] F. Ferrante, N. Armata, G. Lazzara, Modeling of the Halloysite Spiral Nanotube, J. Phys. Chem. C. 119 (2015) 16700–16707. https://doi.org/10.1021/acs.jpcc.5b04281.

[13] V. Vergaro, E. Abdullayev, Y.M. Lvov, A. Zeitoun, R. Cingolani, R. Rinaldi, S. Leporatti, Cytocompatibility and Uptake of Halloysite Clay Nanotubes, Biomacromolecules. 11 (2010) 820–826. https://doi.org/10.1021/bm9014446.

[14] S.R. Levis, P.B. Deasy, Characterisation of halloysite for use as a microtubular drug delivery system, Int. J. Pharm. 243 (2002) 125–134. https://doi.org/10.1016/S0378-5173(02)00274-0.

[15] G. Lazzara, G. Cavallaro, A. Panchal, R. Fakhrullin, A. Stavitskaya, V. Vinokurov, Y. Lvov, An assembly of organic-inorganic composites using halloysite clay nanotubes, Curr. Opin. Colloid Interface Sci. 35 (2018) 42–50. https://doi.org/10.1016/j.cocis.2018.01.002.

[16] H. Zhang, Selective modification of inner surface of halloysite nanotubes: A review, Nanotechnol. Rev. 6 (2017) 573–581. https://doi.org/10.1515/ntrev-2017-0163.
[17] E. Tarasova, E. Naumenko, E. Rozhina, F. Akhatova, R. Fakhrullin, Cytocompatibility and uptake of polycations-modified halloysite clay nanotubes, Appl. Clay Sci. 169 (2019) 21–30. https://doi.org/10.1016/j.clay.2018.12.016.
[18] G. Cavallaro, I. Grillo, M. Gradzielski, G. Lazzara, Structure of Hybrid Materials Based on Halloysite Nanotubes Filled with Anionic Surfactants, J. Phys. Chem. C. 120 (2016) 13492–13502. https://doi.org/10.1021/acs.jpcc.6b01282.
[19] Y.M. Lvov, D.G. Shchukin, H. Möhwald, R.R. Price, Halloysite Clay Nanotubes for Controlled Release of Protective Agents, ACS Nano. 2 (2008) 814–820. https://doi.org/10.1021/nn800259q.
[20] P. Dramou, M. Fizir, A. Taleb, A. Itatahine, N.S. Dahiru, Y.A. Mehdi, L. Wei, J. Zhang, H. He, Folic acid-conjugated chitosan oligosaccharide-magnetic halloysite nanotubes as a delivery system for camptothecin, Carbohydr. Polym. 197 (2018) 117–127. https://doi.org/10.1016/j.carbpol.2018.05.071.
[21] G. Cavallaro, G. Lazzara, S. Milioto, F. Parisi, V. Evtugyn, E. Rozhina, R. Fakhrullin, Nanohydrogel Formation within the Halloysite Lumen for Triggered and Sustained Release, ACS Appl. Mater. Interfaces. 10 (2018) 8265–8273. https://doi.org/10.1021/acsami.7b19361.
[22] C. Duce, V.D. Porta, E. Bramanti, B. Campanella, A. Spepi, M.R. Tiné, Loading of halloysite nanotubes with BSA, α -Lac and β -Lg: a Fourier transform infrared spectroscopic and thermogravimetric study, Nanotechnology. 28 (2017) 055706.
[23] M. Liu, Y. Chang, J. Yang, Y. You, R. He, T. Chen, C. Zhou, Functionalized halloysite nanotube by chitosan grafting for drug delivery of curcumin to achieve enhanced anticancer efficacy, J Mater Chem B. 4 (2016) 2253–2263. https://doi.org/10.1039/C5TB02725J.
[24] Y.-P. Wu, J. Yang, H.-Y. Gao, Y. Shen, L. Jiang, C. Zhou, Y.-F. Li, R.-R. He, M. Liu, Folate-Conjugated Halloysite Nanotubes, an Efficient Drug Carrier, Deliver Doxorubicin for Targeted Therapy of Breast Cancer, ACS Appl. Nano Mater. 1 (2018) 595–608. https://doi.org/10.1021/acsanm.7b00087.
[25] F. Liu, L. Bai, H. Zhang, H. Song, L. Hu, Y. Wu, X. Ba, Smart H2O2-Responsive Drug Delivery System Made by Halloysite Nanotubes and Carbohydrate Polymers, ACS Appl. Mater. Interfaces. 9 (2017) 31626–31633. https://doi.org/10.1021/acsami.7b10867.
[26] Y. Zhang, L. Bai, C. Cheng, Q. Zhou, Z. Zhang, Y. Wu, H. Zhang, A novel surface modification method upon halloysite nanotubes: A desirable cross-linking agent to construct hydrogels, Appl. Clay Sci. 182 (2019) 105259. https://doi.org/10.1016/j.clay.2019.105259.
[27] Y. Darrat, E. Naumenko, G. Cavallaro, G. Lazzara, Y. Lvov, R. Fakhrullin, Tubular Nanocontainers for Drug Delivery, in: Mater. Nanoarchitectonics, Wiley-VCH Verlag GmbH & Co. KGaA, 2018: pp. 85–108. https://doi.org/10.1002/9783527808311.ch4.
[28] A. Spepi, C. Duce, A. Pedone, D. Presti, J.-G. Rivera, V. Ierardi, M.R. Tiné, Experimental and DFT Characterization of Halloysite Nanotubes Loaded with Salicylic Acid, J. Phys. Chem. C. 120 (2016) 26759–26769. https://doi.org/10.1021/acs.jpcc.6b06964.
[29] B. Tang, H. Zhang, C. Cheng, H. Jiang, L. Bai, X. Ba, Y. Wu, Development of halloysite nanotube-based hydrogel with colorimetric H2O2-responsive character, Appl. Clay Sci. 212 (2021) 106230. https://doi.org/10.1016/j.clay.2021.106230.
[30] L. Lisuzzo, G. Cavallaro, S. Milioto, G. Lazzara, Halloysite nanotubes filled with salicylic acid and sodium diclofenac: effects of vacuum pumping on loading and release properties, J. Nanostructure Chem. (2021). https://doi.org/10.1007/s40097-021-00391-z.
[31] M. Tonelli, I. Perini, F. Ridi, P. Baglioni, Improving the properties of antifouling hybrid composites: The use of Halloysites as nano-containers in epoxy coatings, Colloids Surf. Physicochem. Eng. Asp. 623 (2021) 126779. https://doi.org/10.1016/j.colsurfa.2021.126779.

[32] E. Boccalon, G. Viscusi, A. Sorrentino, F. Marmottini, M. Nocchetti, G. Gorrasi, Solvent-free synthesis of halloysite-layered double hydroxide composites containing salicylate as novel, active fillers, Colloids Surf. Physicochem. Eng. Asp. 627 (2021) 127135. https://doi.org/10.1016/j.colsurfa.2021.127135.
[33] P. Pasbakhsh, G.J. Churchman, J.L. Keeling, Characterisation of properties of various halloysites relevant to their use as nanotubes and microfibre fillers, Appl. Clay Sci. 74 (2013) 47–57. https://doi.org/10.1016/j.clay.2012.06.014.
[34] V. Bugatti, G. Viscusi, C. Naddeo, G. Gorrasi, Nanocomposites based on PCL and halloysite nanotubes filled with lysozyme: Effect of draw ratio on the physical properties and release analysis, Nanomaterials. 7 (2017). https://doi.org/10.3390/nano7080213.
[35] G. Gorrasi, Dispersion of halloysite loaded with natural antimicrobials into pectins: Characterization and controlled release analysis, Carbohydr. Polym. 127 (2015) 47–53. https://doi.org/10.1016/j.carbpol.2015.03.050.
[36] G. Gorrasi, V. Bugatti, M. Ussia, R. Mendichi, D. Zampino, C. Puglisi, S.C. Carroccio, Halloysite nanotubes and thymol as photo protectors of biobased polyamide 11, Polym. Degrad. Stab. 152 (2018) 43–51. https://doi.org/10.1016/j.polymdegradstab.2018.03.015.
[37] M. Barman, S. Mahmood, R. Augustine, A. Hasan, S. Thomas, K. Ghosal, Natural halloysite nanotubes /chitosan based bio-nanocomposite for delivering norfloxacin, an anti-microbial agent in sustained release manner, Int. J. Biol. Macromol. 162 (2020) 1849–1861. https://doi.org/10.1016/j.ijbiomac.2020.08.060.
[38] Y. Tian, Q. Qian, Y. Sheng, X. Zhang, H. Wu, L. Xu, L. Li, H. Ye, High energy density in poly(vinylidene fluoride-trifluoroethylene) composite incorporated with modified halloysite nanotubular architecture, Colloids Surf. Physicochem. Eng. Asp. 625 (2021) 126993. https://doi.org/10.1016/j.colsurfa.2021.126993.
[39] J. Raja Beryl, J.R. Xavier, Influence of silane functionalized nanoclay on the barrier, mechanical and hydrophobic properties by clay nanocomposite films in an aggressive chloride medium, Colloids Surf. Physicochem. Eng. Asp. 630 (2021) 127625. https://doi.org/10.1016/j.colsurfa.2021.127625.
[40] T. Selkälä, T. Suopajärvi, J.A. Sirviö, T. Luukkonen, P. Kinnunen, K.I. Kling, J.B. Wagner, H. Liimatainen, Efficient entrapment and separation of anionic pollutants from aqueous solutions by sequential combination of cellulose nanofibrils and halloysite nanotubes, Chem. Eng. J. 374 (2019) 1013–1024. https://doi.org/10.1016/j.cej.2019.06.008.
[41] K. Zhu, Y. Duan, F. Wang, P. Gao, H. Jia, C. Ma, C. Wang, Silane-modified halloysite/Fe3O4nanocomposites: Simultaneous removal of Cr(VI) and Sb(V) and positive effects of Cr(VI) on Sb(V) adsorption, Chem. Eng. J. 311 (2017) 236–246. https://doi.org/10.1016/j.cej.2016.11.101.
[42] Y. Zhao, E. Abdullayev, A. Vasiliev, Y. Lvov, Halloysite nanotubule clay for efficient water purification, J. Colloid Interface Sci. 406 (2013) 121–129. https://doi.org/10.1016/j.jcis.2013.05.072.
[43] M. Omarova, L.T. Swientoniewski, I.K.M. Tsengam, A. Panchal, T. Yu, D.A. Blake, Y.M. Lvov, D. Zhang, V. John, Engineered Clays as Sustainable Oil Dispersants in the Presence of Model Hydrocarbon Degrading Bacteria: The Role of Bacterial Sequestration and Biofilm Formation, ACS Sustain. Chem. Eng. 6 (2018) 14143–14153. https://doi.org/10.1021/acssuschemeng.8b02744.
[44] K. Govindasamy, N.A. Dahlan, P. Janarthanan, K.L. Goh, S.-P. Chai, P. Pasbakhsh, Electrospun chitosan/polyethylene-oxide (PEO)/halloysites (HAL) membranes for bone regeneration applications, Appl. Clay Sci. 190 (2020) 105601. https://doi.org/10.1016/j.clay.2020.105601.
[45] U. Baig, M.A. Gondal, M.A. Dastageer, W.S. Falath, Rapid fabrication of textured membrane with super-wettability using simple spray-coating of Pd-doped WO3 nanoparticles for efficient

oil-water separation, Colloids Surf. Physicochem. Eng. Asp. 609 (2021) 125643. https://doi.org/10.1016/j.colsurfa.2020.125643.
[46] L. Lisuzzo, G. Cavallaro, S. Milioto, G. Lazzara, Halloysite nanotubes as nanoreactors for heterogeneous micellar catalysis, J. Colloid Interface Sci. 608 (2022) 424–434. https://doi.org/10.1016/j.jcis.2021.09.146.
[47] S. Sadjadi, M.M. Heravi, M. Malmir, Pd@HNTs-CDNS-g-C3N4: A novel heterogeneous catalyst for promoting ligand and copper-free Sonogashira and Heck coupling reactions, benefits from halloysite and cyclodextrin chemistry and g-C3N4 contribution to suppress Pd leaching, Carbohydr. Polym. 186 (2018) 25–34. https://doi.org/10.1016/j.carbpol.2018.01.023.
[48] Y. Liu, J. Zhang, H. Guan, Y. Zhao, J.-H. Yang, B. Zhang, Preparation of bimetallic Cu-Co nanocatalysts on poly (diallyldimethylammonium chloride) functionalized halloysite nanotubes for hydrolytic dehydrogenation of ammonia borane, Appl. Surf. Sci. 427 (2018) 106–113. https://doi.org/10.1016/j.apsusc.2017.08.171.
[49] Y. Liu, H. Guan, J. Zhang, Y. Zhao, J.-H. Yang, B. Zhang, Polydopamine-coated halloysite nanotubes supported AgPd nanoalloy: An efficient catalyst for hydrolysis of ammonia borane, Int. J. Hydrog. Energy. 43 (2018) 2754–2762. https://doi.org/10.1016/j.ijhydene.2017.12.105.
[50] S. Sadjadi, G. Lazzara, M.M. Heravi, G. Cavallaro, Pd supported on magnetic carbon coated halloysite as hydrogenation catalyst: Study of the contribution of carbon layer and magnetization to the catalytic activity, Appl. Clay Sci. 182 (2019) 105299. https://doi.org/10.1016/j.clay.2019.105299.
[51] D. Jiang, H. Jing, Z. Liu, C. Jia, Q. Liu, Natural Halloysite Nanotube as a Spatially Confined Nanoreactor for Improving Photocatalytic Performance, J. Phys. Chem. C. 125 (2021) 15316–15323. https://doi.org/10.1021/acs.jpcc.1c04065.
[52] A. Glotov, A. Vutolkina, A. Pimerzin, V. Vinokurov, Y. Lvov, Clay nanotube-metal core/shell catalysts for hydroprocesses, Chem Soc Rev. 50 (2021) 9240–9277. https://doi.org/10.1039/D1CS00502B.
[53] A. Stavitskaya, K. Mazurova, M. Kotelev, O. Eliseev, P. Gushchin, A. Glotov, R. Kazantsev, V. Vinokurov, Y. Lvov, Ruthenium-Loaded Halloysite Nanotubes as Mesocatalysts for Fischer–Tropsch Synthesis, Molecules. 25 (2020). https://doi.org/10.3390/molecules25081764.
[54] Y. Lvov, A. Panchal, Y. Fu, R. Fakhrullin, M. Kryuchkova, S. Batasheva, A. Stavitskaya, A. Glotov, V. Vinokurov, Interfacial Self-Assembly in Halloysite Nanotube Composites, Langmuir. 35 (2019) 8646–8657. https://doi.org/10.1021/acs.langmuir.8b04313.
[55] G. Cavallaro, S. Milioto, S. Konnova, G. Fakhrullina, F. Akhatova, G. Lazzara, R. Fakhrullin, Y. Lvov, Halloysite/Keratin Nanocomposite for Human Hair Photoprotection Coating, ACS Appl. Mater. Interfaces. 12 (2020) 24348–24362. https://doi.org/10.1021/acsami.0c05252.
[56] A. Panchal, G. Fakhrullina, R. Fakhrullin, Y. Lvov, Self-assembly of clay nanotubes on hair surface for medical and cosmetic formulations, Nanoscale. 10 (2018) 18205–18216. https://doi.org/10.1039/C8NR05949G.
[57] I. Fatimah, Preparation, characterization and physicochemical study of 3-amino propyl trimethoxy silane-modified kaolinite for Pb(II) adsorption, J. King Saud Univ. - Sci. 30 (2018) 250–257. https://doi.org/10.1016/j.jksus.2017.04.006.
[58] R. Duarte-Silva, M.A. Villa-García, M. Rendueles, M. Díaz, Structural, textural and protein adsorption properties of kaolinite and surface modified kaolinite adsorbents, Appl. Clay Sci. 90 (2014) 73–80. https://doi.org/10.1016/j.clay.2013.12.027.
[59] M. Catauro, Thermal and microbiological performance of metakaolin-based geopolymers cement with waste glass, Appl. Clay Sci. (2020) 9.
[60] X. Liu, J. Jiang, H. Zhang, M. Li, Y. Wu, L. Guo, W. Wang, P. Duan, W. Zhang, Z. Zhang, Thermal stability and microstructure of metakaolin-based geopolymer blended with rice husk ash, Appl. Clay Sci. 196 (2020) 105769. https://doi.org/10.1016/j.clay.2020.105769.

[61] G. Cavallaro, L. Chiappisi, P. Pasbakhsh, M. Gradzielski, G. Lazzara, A structural comparison of halloysite nanotubes of different origin by Small-Angle Neutron Scattering (SANS) and Electric Birefringence, Appl. Clay Sci. 160 (2018) 71–80. https://doi.org/10.1016/j.clay.2017.12.044.
[62] G. Cavallaro, G. Lazzara, V. Taormina, D. Cascio, Sedimentation of halloysite nanotubes from different deposits in aqueous media at variable ionic strengths, Colloids Surf. Physicochem. Eng. Asp. 576 (2019) 22–28. https://doi.org/10.1016/j.colsurfa.2019.05.038.
[63] F. Tardani, S. Casciardi, B. Ruzicka, S. Sennato, Salt enhanced sedimentation of halloysite nanotubes for precise determination of DNA adsorption isotherm, Colloids Surf. Physicochem. Eng. Asp. 605 (2020) 125400. https://doi.org/10.1016/j.colsurfa.2020.125400.
[64] B. Katana, D. Takács, E. Csapó, T. Szabó, A. Jamnik, I. Szilagyi, Ion Specific Effects on the Stability of Halloysite Nanotube Colloids—Inorganic Salts versus Ionic Liquids, J. Phys. Chem. B. 124 (2020) 9757–9765. https://doi.org/10.1021/acs.jpcb.0c07885.
[65] X. Kang, Z. Xia, R. Chen, P. Liu, W. Yang, Effects of inorganic cations and organic polymers on the physicochemical properties and microfabrics of kaolinite suspensions, Appl. Clay Sci. 176 (2019) 38–48. https://doi.org/10.1016/j.clay.2019.04.024.
[66] T. Nasim, A. Pal, A. Bandyopadhyay, Flocculation of aqueous kaolin suspension using a biodegradable flocculant system of poly (vinyl alcohol)-Acacia nilotica gum blends, Appl. Clay Sci. 152 (2018) 83–92. https://doi.org/10.1016/j.clay.2017.10.035.
[67] J. Cao, X. Kang, B. Bate, Microscopic and physicochemical studies of polymer-modified kaolinite suspensions, Colloids Surf. Physicochem. Eng. Asp. 554 (2018) 16–26. https://doi.org/10.1016/j.colsurfa.2018.06.019.
[68] E.I. Benítez, D.B. Genovese, J.E. Lozano, Effect of typical sugars on the viscosity and colloidal stability of apple juice, Food Hydrocoll. 23 (2009) 519–525. https://doi.org/10.1016/j.foodhyd.2008.03.005.
[69] I. Blanco, G. Cicala, A. Latteri, G. Saccullo, A.M.M. El-Sabbagh, G. Ziegmann, Thermal characterization of a series of lignin-based polypropylene blends, J. Therm. Anal. Calorim. 127 (2017) 147–153. https://doi.org/10.1007/s10973-016-5596-2.
[70] I. Blanco, G. Cicala, C. Tosto, F.A. Bottino, Kinetic Study of the Thermal and Thermo-Oxidative Degradations of Polystyrene Reinforced with Multiple-Cages POSS, Polymers. 12 (2020) 2742. https://doi.org/10.3390/polym12112742.
[71] C. Cionti, T. Taroni, V. Sabatini, D. Meroni, Nanostructured Oxide-Based Systems for the pH-Triggered Release of Cinnamaldehyde, Materials. 14 (2021). https://doi.org/10.3390/ma14061536.
[72] C. Duce, S. Vecchio Ciprioti, L. Ghezzi, V. Ierardi, M. Tinè, Thermal behavior study of pristine and modified halloysite nanotubes, J. Therm. Anal. Calorim. 121 (2015) 1011–1019. https://doi.org/10.1007/s10973-015-4741-7.
[73] G. Cavallaro, G. Lazzara, S. Milioto, Exploiting the Colloidal Stability and Solubilization Ability of Clay Nanotubes/Ionic Surfactant Hybrid Nanomaterials, J. Phys. Chem. C. 116 (2012) 21932–21938. https://doi.org/10.1021/jp307961q.
[74] M. Wojdyr, ıt Fityk: a general-purpose peak fitting program, J. Appl. Crystallogr. 43 (2010) 1126–1128. https://doi.org/10.1107/S0021889810030499.